Tech Science Press

check for updates

Optimal Deep Learning Model Enabled Secure UAV Classification for Industry 4.0

Khalid A. Alissa[1], Mohammed Maray[2], Areej A. Malibari[3], Sana Alazwari[4], Hamed Alqahtani[5], Mohamed K. Nour[6], Marwa Obbaya[7], Mohamed A. Shamseldin[8] and Mesfer Al Duhayyim[9,*]

[1]SAUDI ARAMCO Cybersecurity Chair, Networks and Communications Department, College of Computer Science and Information Technology, Imam Abdulrahman bin Faisal University, P.O. Box 1982, Dammam, 31441, Saudi Arabia
[2]Department of Information Systems, College of Computer Science, King Khalid University, Abha, Saudi Arabia
[3]Department of Industrial and Systems Engineering, College of Engineering, Princess Nourah bint Abdulrahman University, P.O. Box 84428, Riyadh, 11671, Saudi Arabia
[4]Department of Information Technology, College of Computers and Information Technology, Taif University, Taif P.O. Box 11099, Taif, 21944, Saudi Arabia
[5]Department of Information Systems, College of Computer Science, Center of Artificial Intelligence, Unit of Cybersecurity, King Khalid University, Abha, Saudi Arabia
[6]Department of Computer Sciences, College of Computing and Information System, Umm Al-Qura University, Saudi Arabia
[7]Department of Biomedical Engineering, College of Engineering, Princess Nourah bint Abdulrahman University, P.O. Box 84428, Riyadh, 11671, Saudi Arabia
[8]Department of Mechanical Engineering, Faculty of Engineering and Technology, Future University in Egypt, New Cairo, 11835, Egypt
[9]Department of Computer Science, College of Sciences and Humanities- Aflaj, Prince Sattam bin Abdulaziz University, Saudi Arabia
*Corresponding Author: Mesfer Al Duhayyim. Email: m.alduhayyim@psau.edu.sa
Received: 20 June 2022; Accepted: 28 September 2022

Abstract: Emerging technologies such as edge computing, Internet of Things (IoT), 5G networks, big data, Artificial Intelligence (AI), and Unmanned Aerial Vehicles (UAVs) empower, Industry 4.0, with a progressive production methodology that shows attention to the interaction between machine and human beings. In the literature, various authors have focused on resolving security problems in UAV communication to provide safety for vital applications. The current research article presents a Circle Search Optimization with Deep Learning Enabled Secure UAV Classification (CSODL-SUAVC) model for Industry 4.0 environment. The suggested CSODL-SUAVC methodology is aimed at accomplishing two core objectives such as secure communication via image steganography and image classification. Primarily, the proposed CSODL-SUAVC method involves the following methods such as Multi-Level Discrete Wavelet Transformation (ML-DWT), CSO-related Optimal Pixel Selection (CSO-OPS), and signcryption-based encryption. The proposed model deploys the CSO-OPS technique to select the optimal pixel points in cover images. The secret images, encrypted by signcryption technique, are embedded into cover images. Besides, the image classification process includes

three components namely, Super-Resolution using Convolution Neural Network (SRCNN), Adam optimizer, and softmax classifier. The integration of the CSO-OPS algorithm and Adam optimizer helps in achieving the maximum performance upon UAV communication. The proposed CSODL-SUAVC model was experimentally validated using benchmark datasets and the outcomes were evaluated under distinct aspects. The simulation outcomes established the supreme better performance of the CSODL-SUAVC model over recent approaches.

1 Introduction

Recent technological advancements such as Artificial Intelligence (AI), Edge Computing, 5G, Internet of Things (IoT), and big data analytics are incorporated in industries with innovation and cognitive skills. These cutting-edge technologies might be helpful for industries to rapidly escalate their manufacturing and delivery processes and customization of their goods [1]. Such enabling technologies empower Industry 4.0 with advanced production models that enable communication between humans and machines. In the smart machinery concept, both humans and machines co-work together and this phenomenon improves the capabilities of human beings effectively. Further, smart machinery was innovated to automate processes, persons, and industries at a given time [2]. According to Industry 4.0, the automation processes and the launch of edge computing occur in a dispersed and intellectual manner. The primary goal is to enhance the potentiality of the processes, thereby unintentionally avoiding the human cost incurred upon the maximization of the processes [3]. Fig. 1 showcases the types of industrial versions.
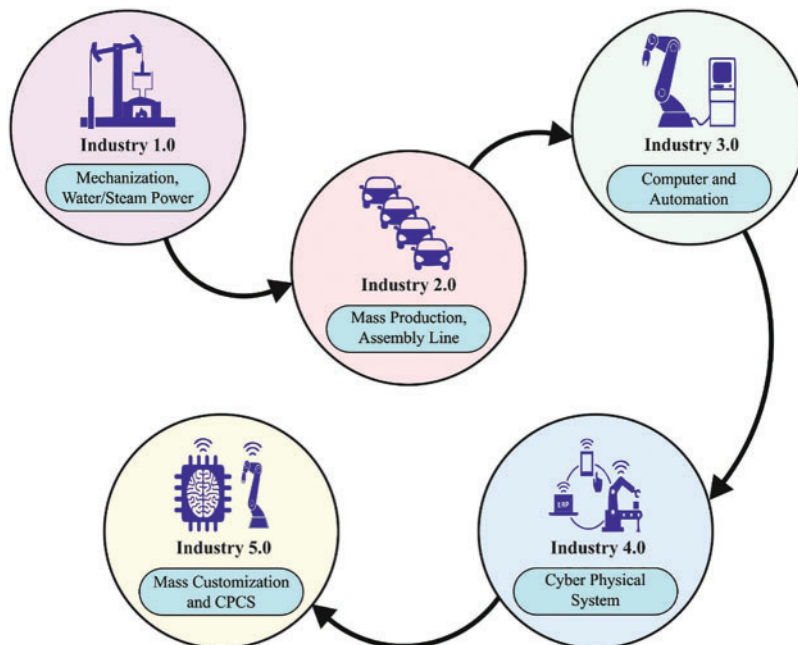
Figure 1: Types of industrial versions

On the other hand, avoiding or reducing manpower in industries will become a huge issue in the upcoming years, when Industry 4.0 becomes fully operative. Further, it would also face opposition from politicians and labor unions to compromise on the advantages of Industry 4.0 to improve employment opportunities [4,5]. But there is no need to reverse the evolution of the Industry 4.0 concept since process effectiveness should be improved by launching modern technology continuously. It can be suggested that Industry 4.0 can be considered to be a viable solution and it is required after the backward push commences [6]. Industry 4.0 can be expected to put forward a complete structure for automated and linked systems that range from individual cars to Unmanned Aerial Vehicles (UAV), with different necessities in terms of reliability, latency, energy efficiency, and data rate. Drones, on the other hand, serve a significant portion in wide scenarios that might surpass 6G and 5G too [7].

Owing to their adaptability, automation abilities, and less cost, drones have been extensively applied to meet civilian needs in the past few years [8]. Some of the instances include precision agriculture, power line inspection, building inspection, and wildlife conservation [9]. But, drones have a set of restrictions in terms of weight, size, energy utilization of the payload, restricted range of operations, and endurance. Such limits should not be ignored, especially when Deep Learning (DL) systems are required to be run on board [10]. Aerial imagery classification of scenes classifies the aerial images, captured using drones, to sub-areas, by masking several ground matters and types of land covers, to numerous semantic forms. In many real-time implications such as urban planning, computer cartography, and the management of remote sensing sources, aerial image classifier plays a significant role [11,12]. This approach is highly efficient in most domains, especially in educational and industrial settings, than the standard processes [13]. DL method endeavors to extract some of the commonly available hierarchies of Feature Learning (FL) concerning numerous abstraction stages. Deep Convolutional Neural Network (CNN) is the most commonly applied DL technique [14]. This method has become familiar and successful in countless detection and recognition tasks, receiving superior outcomes over a count of standard datasets.

The current research article presents a Circle Search Optimization with Deep Learning Enabled Secure UAV Classification (CSODL-SUAVC) model for Industry 4.0 environment. The proposed CSODL-SUAVC technique consists of Multi-Level Discrete Wavelet Transformation (ML-DWT), CSO-related Optimal Pixel Selection (CSO-OPS), and signcryption-based encryption. Besides, the image classification process includes three components such as Super-Resolution using Convolution Neural Network (SRCNN), Adam optimizer, and softmax classifier. The proposed CSODL-SUAVC method was experimentally validated using benchmark datasets and the outcomes were assessed under distinct aspects.

2 Literature Review

The aim of the study conducted earlier [15] was to provide a survey-related tutorial on potential applications and support technologies for Industry 4.0. At first, the researchers presented a new concept and defined Industry 4.0 from the perspectives of industrial practitioners and researchers. Next, the research scholars elaborated on the potential applications of Industry 4.0 such as cloud manufacturing, intellectual healthcare, manufacturing production, and supply chain management. In the literature [16], the authors continuously monitored the harmful gas to alert the people, in case of any leakage, and to save them from accidents. Further, the study also discussed Industry 4.0 from the perspective of leveraging UAV's longer-range transmission.

Bhat et al. [17] proposed Agri-SCM-BIoT (Agriculture Supply Chain Management utilizing Blockchain and IoT) structure and deliberated the classification of security threats with IoT architecture and the existing blockchain-related defense mechanisms. In the study conducted earlier [18], the researchers presented a Machine Learning (ML)-based architecture for rapid identification and detection of UAE over encrypted Wi-Fi traffic. The architecture was inspired by the observations made when a consumer UAV uses a Wi-Fi link for controlling and video streaming purposes [19]. In this study, the significance of a secure drone network was emphasized in terms of preventing intrusion and interception. A hybrid ML method was developed, combining Logistic Regression (LR) and Random Forest (RF) methods, to categorize the data instances for maximum effectiveness. By integrating the sophisticated AI-stimulated approaches with NoD architecture, the presented method mitigated the cybersecurity vulnerabilities with the creation of secure NoD security and its protection.

In literature [20], the authors proposed an autonomous Intrusion Detection System (IDS) that can effectively recognize the malicious threats which invade UAVs with Deeper Convolution Neural Network (UAV-IDS-ConvNet). Especially, the presented method considered the encryption of the Wi-Fi traffic dataset collected from three different kinds of widely-employed UAVs. Kumar et al. [21] presented a Secured Privacy-Preserving Framework (SP2F) for smart agriculture UAVs. The presented SP2F architecture had two major engines such as a two-level privacy engine and a DL-related anomaly detection engine. In this method, SAE was employed to transform the information into a novel encoded format to prevent inference attacks.

3 The Proposed Model

In this article, a novel CSODL-SUAVC algorithm has been developed to accomplish secure UAV classification and communication in the Industry 4.0environment. The presented CSODL-SUAVC technique performs image steganography via ML-DWT, CSO-related optimal pixel selection, and signcryption base- encryption technique. At the same time, the image classification module encompasses SRCNN-based feature extraction, Adam optimizer, and softmax classifier. Fig. 2 depicts the block diagram of the proposed CSODL-SUAVC approach.

3.1 Secure UAV Communication Module

To accomplish secure UAV communication, the proposed model deploys the CSO-OPS technique to select the optimal pixel points in a cover image. Then, the secret image, encrypted by the signcryption technique, is embedded onto the cover image.

3.1.1 Image Decomposition

RGB cover images are classified based on Low High (LH), High Low (HL), Low Low (LL), and High High (HH) frequency bands to find the location of a pixel. Here, 2D-DWT is the prominent spatial applied in the frequency domain conversion model [22]. When an image is partitioned, it follows horizontal and vertical processes. The vertical function decomposes the images to HH_1, LL_1, LH_1, and HL_1 frequency bands. Then, the horizontal function decomposes the images into High (H) and Low (L) bands. To follow the decomposition process, LL_1 the band gets decomposed into LL_2, LH_2, HL_2, and HH_2. Here, the image size indicates 'M∗N'. At first, to filter and down-sample the images, the

horizontal one reduces the size of the image to $M \times \dfrac{N}{2}$. The vertical decomposition reduces the down-sampling of the image size to $\dfrac{M}{2} \times \dfrac{N}{2}$. A single-level decomposition outcome is achieved using the following equation.

$$[C_1 C_2 C_3 C_4] = \text{DWT}(C) \tag{1}$$
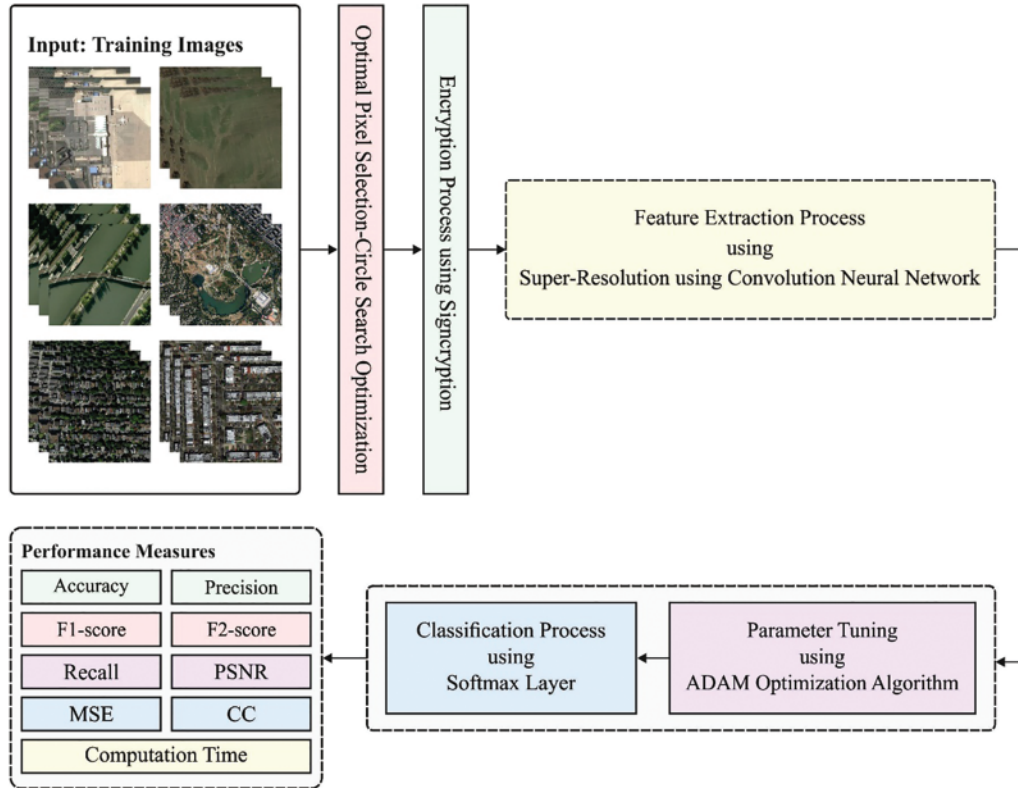
Figure 2: Block diagram of CSODL-SUAVC approach

In Eq. (1), 'C_1', 'C_2', 'C_3', and 'C_4' represent the co-efficient values of the decomposing frequency band. 'C_1' represents the low frequency band that gets decomposed to create further sub-bands as given herewith.

$$\left[C_1^{LL1} C_1^{LH1} C_1^{HL1} C_1^{HH1}\right] = \text{DWT}(C_1) \tag{2}$$

The co-efficient in the lower level band C_1^{LL1} gets completely decomposed, because it generates the texture as well as the edge details of the images. The subsequent decomposition, as expressed in Eq. (3) is implemented on the low band, LL_1.

$$\left[C_1^{LL2} C_1^{LH2} C_1^{HL2} C_1^{HH2}\right] = \text{DWT}(LL_1) \tag{3}$$

In Eq. (3), C_1^{LL2} indicates the low-frequency band of the following decomposition.

3.1.2 Optimal Pixel Selection Process

CSO algorithm is applied in this stage to select the optimal pixels of the images. The geometrical circle is an underlying closed curve that has a similar distance from the center to every point [23]. The diameter is calculated as a line, connecting two points on a curve that intersect at the (x_c) center. Radius (R) refers to the line that connects some points in a circle, towards the center. As per the Pythagorean equation, the orthogonal function (Tan) of the right triangle has a ratio between the perpendicular tangent line segment and the radius. The radius can be determined only through the distance between x_t and x_C. The tangent line segment can be determined as a measure of distance between x_t and x_p points whereas the orthogonal function (Tan) can be formulated using the subsequent expression:

$$Tan\,(\theta) = \frac{\chi_t - x_c}{x_p - x_t} \tag{4}$$

$$x_t - x_c = (x_p - x_t) \times Tan\,(\theta) \tag{5}$$

$$x_t = x_c + (x_p - x_t) \times Tan\,(\theta) \tag{6}$$

CSO seeks an optimal answer inside a random circle to widen the possibilities of the searching region. By utilizing the center of the circle as a target point, the circumference of the circle and the angle of contacting points of the tangent line reduce gradually, until it approaches the center of the circle. Owing to the probability that this circle gets stuck with the local solution, the angle, where the tangent line touches the point, is randomly changed. The X_t touching point considers the searching agent of the CSO whereas X_c denotes that the center point is regarded as the optimum location. CSO upgrades the searching agent for the movement of the touching point towards the center. Nonetheless, to avoid CSO from getting trapped in a local solution, the contact point is randomly upgraded by altering its angle. The key steps of the CSO optimizer are shown herewith.

Step 1: Initialization: This is a crucial phase in CSO in which the overall set of the dimensions of the searching agent must be randomized equally, as demonstrated in Algorithm 1. The majority of the existing codes randomize the dimension unequally. This phenomenon occasionally makes the algorithm achieve a better outcome unexpectedly. Next, the searching agent is initialized between the (UB) and (LB) upper and lower limits of the searching region as given below.

$$X_t = LB + r \times (UB - LB) \tag{7}$$

In Eq. (7), the random vector is represented by r and its value lies in the range of 0 and 1.

Step 2: Upgrade the location of the searching agent; the location of the searching agent X_t is upgraded based on the assessed optimal position X_c as follows.

$$X_t = X_c + (X_c - X_t) \times \tan\,(\theta) \tag{8}$$

In Eq. (8), angle θ plays an essential role in both the exploitation and exploration phases of CSO and is evaluated using the following expression

$$\theta = \begin{cases} w \times rand & Iter > (c \times Ma\chi iter)(\textit{escape from local stagnation}) \\ w \times p & \textit{otherwise} \end{cases} \tag{9}$$

$$w = w \times rand - w \tag{10}$$

$$a = \pi - \pi \times \left(\frac{Iter}{Max\ iter}\right)^2 \tag{11}$$

$$p = 1 - 0.9 \times \left(\frac{Iter}{Max\ iter}\right)^{0.5} \tag{12}$$

In this expression, the random number is represented by rand that lies in the range of 0 and 1. Iter refers to the iteration count, Maxiter indicates the maximal iteration amount, and c denotes a constant that lies within the interval of [0,1] and characterizes the percentage of maximal iteration. Eq. (10) demonstrates that w variable varies from $[-\pi, 0]$ with an increasing number of iterations. The parameter a differs from $[\pi, 0]$, based on Eq. (11). The parameters p varies between [1,0] as shown in Eq. (12). Consequently, the angle θ differs between $[-\pi, 0]$.

Algorithm 1: Initialization of CSO

Input LB and UB.
Do for every searching agent
r =random value from [0, 1].
Utilize Eq. (4) for initializing X_t the searching agent.
End Do
Algorithm 2 Pseudocode of CSO
Initializes the searching agent X_t by utilizing Algorithm 1
Input the constant value, $Iter = 0$, and Maxi
Whereas Iter is lesser than Maxiter
Use Eq. (11) for finding the value of a
Do for each searching agent
Utilize Eq. (10) for finding the value of w
Utilize Eq. (12) for finding the value of p
Utilize Eq. (9) for finding the value of angle θ
Utilize Eq. (8) for updating the search agent X_t
Once the upgrade searching agent is out of the boundary, the set searching agent is equivalent to the boundary defining the fitness function $f(X_t)$
End Do
Estimate the $f(X_t)$ with the storing optimal solutions $f(X_c)$ Upgrade $f(X_c)$ and X_c
$$Iter = Iter + 1$$

End While
Output $f(X_c)$ and X_c

Fitness Function is used to evaluate the objective function. The primary intention is to design a steganography model that must maximize PSNR and minimize the error rate (MSE) and is achieved using the following equation.

$$F = \{\min(MSE), \max(PSNR)\} \tag{13}$$

Both maximized and minimized values can be acquired by leveraging the CSO system.

3.1.3 Encryption Process

The proposed model enables an encryption approach to encrypt secret images. Signcryption is a public key cryptosystem that provides sufficient privacy to private images, by producing digital signatures and following the encryption process. The parameter, utilized in the Signcryption technique, is denoted by standard 'cp' while 'xs' denotes the private key of the sender, 'S' denotes the sender, 'ys' denotes the sender and receiver public key, and the public key of the receiver is denoted by 'yr'. While 'yr' is fed as input in the form of 'binfo' to the Signcryption system. The variable 'binfo' is fundamental to secure the Signcryption process and is composed of strings that exclusively recognize the receiver and the sender or the hash value of the public key. The steps that are used to signcrypt the private images are discussed below.

Step 1: Choose any value for 'x' in the range of 1 to $L_n - 1$.

Step 2: The hash function is evaluated to receive the public key and 'N' with $K = as(ybx \ mod \ p)$. This creates 128-bit strings.

Step 3: Then, it is segregated into two 64-bit strings such as K1 and K2 (key pairs).

Step 4: The message 'm' is encrypted, through the sender, using a public key encryption system 'E' in which key K1 is used to achieve the cipher text 'c'; here, $c = EK1(m)$.

Step 5: K2 is utilized in a one-way keyed hash 'KH' to retrieve the hash of messages. Here, 'r' represents the hash value of 128 bits for the message $r = KHK2(m)$.

Step 6: Next, the value of 's' is calculated based on the 'x' value and the private key, 'xa' while a large prime value Ln and 'r' are used in s = x/(r + xa) mod Ln

Step 7: c, s, and r values are transferred to the receivers at once via signcryptext 'C' to complete the secured communication.

At last, the encrypted cover image is embedded as an optimal designated pixel point of the cover images. This guarantees the privacy of the stego images, due to the encryption process and the embedding of private images.

3.2 UAV Image Classification Module

To perform UAV image classification, the CSODL-SUAVC model carries out three sub-processes namely, SRCNN-based feature extraction, Adam optimizer, and softmax classifier. There has been some research conducted on utilizing the DL technique for high image resolution [24]. To be specific, SRCNN directly learns end-to-end mappings between higher and lower-resolution images. Mapping signifies a deep-CNN model that comprises non-linear mapping, reconstruction, extraction of the patches, and representation. At the beginning of describing all the operations, only a single low-resolution image is considered. The selected image is then up-scaled towards the preferred size with the help of bi-cubic interpolation; later the image is represented as an interpolated image i.e., $y \in \mathbb{R}^{m \times m \times c}$; at last, it is expected to recover an image $f(y)$ from y viz. same as high-resolution images, $x \in \mathbb{R}^{m \times m \times c}$. Here, y denotes the low-resolution image and x represents the high-resolution image and these notations are used to keep the subsequent representation, simple and understandable.

At first, patch extraction and representation are formulated as given herewith.

$$f_1(y) = \max(0, W_1 \otimes y + b_1) \tag{14}$$

In Eq. (14), W_1 and b_1 represent the filter and bias correspondingly. Specially, W_1 corresponds to $n1$ filter of the support $p_1 \times p_1 \times c$, while c denotes the channel count in input low-resolution image, $y \in \mathbb{R}^{m \times m \times c}$ and p_1 indicates the spatial size of the filter. The bias $b_1 \in \mathbb{R}^{n_1}$. After using the ReLU function $(\max(O, \cdot))$ on filter response, the output $f_1(y)$ is attained from n_1 feature map, viz., $f_1(y) \in \mathbb{R}^{m \times m \times n_1}$.

Next, the nonlinear mapping is expressed as follows.

$$f_2(y) = \max(0, W_2 \otimes f_1(y) + b_2) \tag{15}$$

In Eq. (15), W_2 comprises of an $n2$ filter sized at $p_2 \times p_2 \times n1$ and $b_2 \in \mathbb{R}^{n_2}$. Without losing the generalization norm, it has the potential to add further convolution layers to increase the nonlinearity. The same procedure is repeated with the preceding operation, viz., $f_2(y) \in \mathbb{R}^{m \times m \times n_2}$. Then, for the reconstruction procedure, the last high-resolution image is equated as follows,

$$f_3(y) = W_3 \otimes f_2(y) + b_3 \tag{16}$$

In Eq. (16), W_3 contains a c filter sized at $p_3 \times p_3 \times n2$ and $b_3 \in \mathbb{R}^c$. The procedure is repeated with the preceding operation, viz, $f_3(y) \in \mathbb{R}^{m \times m \times c}$. Even though the abovementioned operation is inspired by diverse intuitions, it produces a similar result in the form of a convolution layer. Furthermore, the filtering weight and bias are enhanced with the help of the subsequent loss function,

$$L(\Theta) = \frac{1}{N} \sum_{n=1}^{N} \|F(y_n, \Theta) - x_n\|_2^2 \tag{17}$$

In Eq. (17), the number of trained instances is represented by N and parameter $\Theta = \{W_1, W_2, W_3, b_1, b_2, b_3\}$. We have $(y, \Theta) \triangleq f_3(y)$.

SM classifier is used to allocate the class labels to the input UAV images.

It multiplies every value obtained irrespective of its nature and converts it to an entire number that is continuously between *zero* and one. It can be a probabilistic function too that adapts a vector distribution of numbers, probability distributing to real distribution. It is a classification that is utilized to validate the accuracy of the model. Here, softmax is determined using the formula given below.

$$\sigma(\vec{z})_i = \frac{e^{z_i}}{\sum_{j=1}^{K} e^{z_j}} \tag{18}$$

whereas, $\sigma = soft \max$

$$\vec{z} = input\ vector \tag{19}$$

e^{z_i} refers to the standard exponential function of input vector K that signifies the number of classes from multi-class classification

e^{z_j} implies the standard exponential function of the resultant vector e^{z_j} which implies the standard exponential function to the resultant vector.

To improve the performance of the SRCNN algorithm, the Adam optimizer is employed. Adam is an optimized approach that is utilized for iteratively upgrading the network weight with the help of trained data, instead of the standard Stochastic Gradient Descent (SGD) process. This method is the most effective technique in overcoming difficult issues with a huge number of variables or data. It is effectual and economical in terms of memory. It performs a mix of Gradient Descent (GD) with

momentum and Root Mean Square propagation techniques [25]. Two GD techniques are integrated into the Adam optimizer. Adam optimizer includes the strength of two preceding methods to further effectual GD. When the formulas are utilized in the two preceding manners, the following equation is obtained.

$$m_t = \beta_1 m_{t-1} + (1 - \beta_1) \left[\frac{\delta L}{\delta w_t} \right] v_t = \beta_2 v_{t-1} + (1 - \beta_2) \left[\frac{\delta L}{\delta w_t} \right]^2 \tag{20}$$

After all the iterations are over, it is instinctively altered to GD thereby remaining constant and impartial across the procedure, and is given the name, Adam. At this point, rather than the normal weighted parameters, m_t and v_t, it can proceed as the bias-corrected weighted parameter. When this information is used as a common formula, the following Eq. (21) can be obtained.

$$w_{t+1} = w_t - \widehat{m}_t \left(\frac{\alpha}{\sqrt{\widehat{v}_t + \varepsilon}} \right) \tag{21}$$

During every technique, this optimization is utilized due to its maximal efficacy and less memory utilization requirement.

4 Result and Discussion

In this section, the proposed CSODL-SUAVC approach was experimentally validated utilizing UCM [26] and AID datasets. A few sample images are shown in Fig. 3. UCM dataset comprises 21 scene types like oil tanks, residential areas, farmland, forest, and so on. There are 100 images present for every scene type and are sized at 256×256 pixels. Altogether, this dataset has 2,100 RGB images with a spatial resolution of $\sim$0.3 m. AID dataset covers 30 scene types with finely classified scene types. The number of RGB images in every category varies in the range of $\sim$220 to 440 RGB images. So, the total amount of images in this dataset is 10,000. The image size is 600×600 pixels and its resolution is $\sim$0.5–8 m.

Table 1 provides the analytical results of the proposed CSODL-SUAVC system and other existing models in terms of MSE and PSNR [27]. Fig. 4 portrays the Mean Square Error (MSE) scrutinization, performed by the CSODL-SUAVC system and other recent models under a distinct number of samples. The figure indicates that the proposed CSODL-SUAVC method gained effectual outcomes with minimal values of MSE. For example, in sample 1, the CSODL-SUAVC model offered a low MSE of 0.049, but other techniques such as AI-based UAV (AIUAV), Cuckoo Search (CS), and Grey Wolf Optimization (GWO) techniques attained high MSE values such as 0.069, 0.108, and 0.164 correspondingly. In addition, in sample 5, the proposed CSODL-SUAVC approach obtained a low MSE of 0.121, where AIUAV, CS, and GWO techniques obtained high MSE values such as 0.138, 0.206, and 0.253 correspondingly.

Figure 3: Sample images

Table 1: Results of the analysis of the CSODL-SUAVC approach on distinct test samples under different measures

Test samples	CSODL-SUAVC		AIUAV model		Cuckoo search algorithm		Grey wolf algorithm	
	MSE	PSNR	MSE	PSNR	MSE	PSNR	MSE	PSNR
Sample 1	0.049	61.229	0.069	60.807	0.108	57.80	0.164	55.98
Sample 2	0.062	60.207	0.081	59.380	0.136	56.80	0.188	55.39
Sample 3	0.037	62.449	0.054	61.796	0.104	57.96	0.151	56.34
Sample 4	0.119	57.375	0.132	57.162	0.192	55.30	0.238	54.37
Sample 5	0.121	57.303	0.138	57.059	0.206	54.99	0.253	54.10
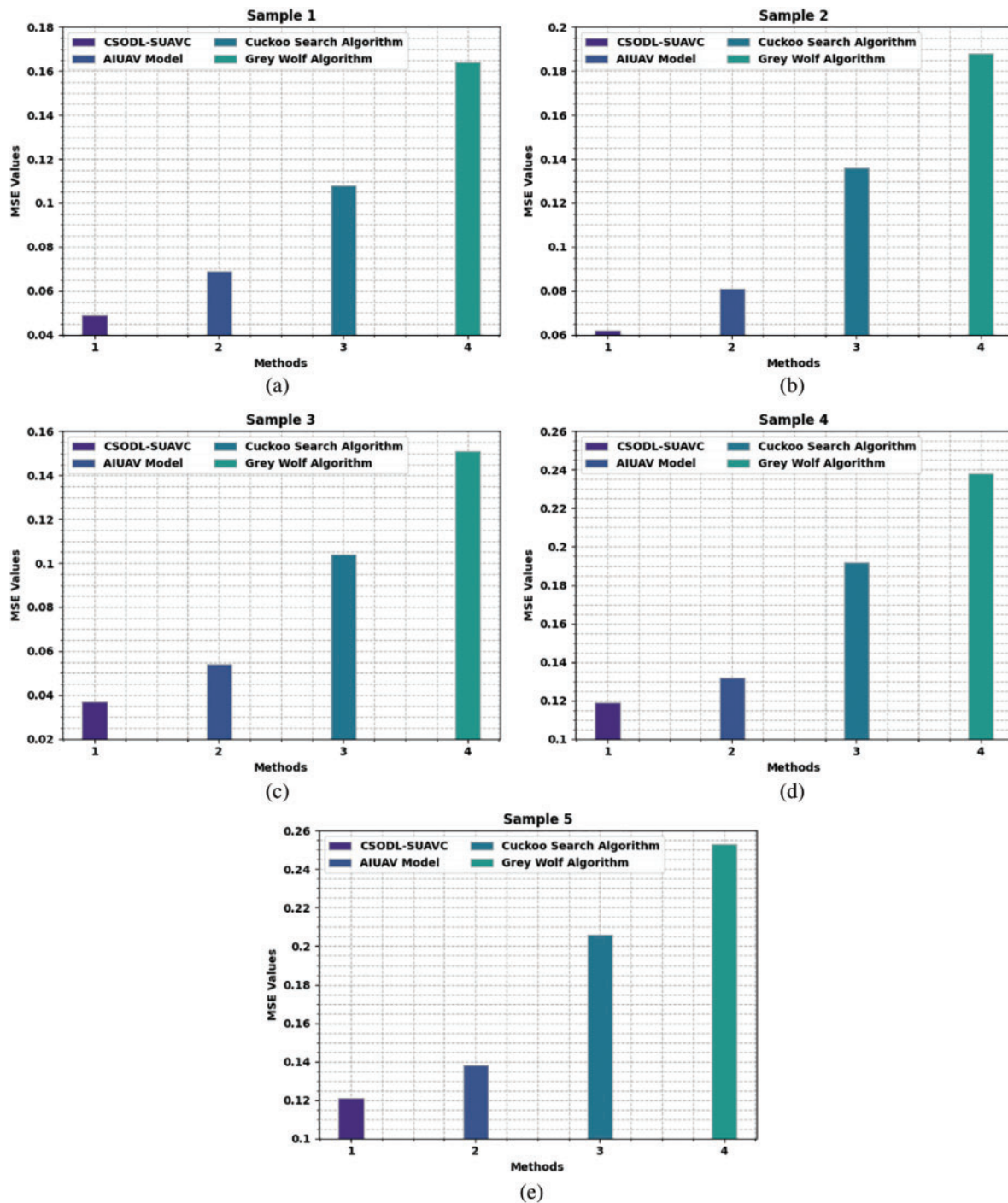
Figure 4: MSE analysis results of CSODL-SUAVC approach (a) Sample 1, (b) Sample 2, (c) Sample 3, (d) Sample 4, and (e) Sample 5

A comparative Peak Signal to Noise Ratio (PSNR) study was conducted on the CSODL-SUAVC model and other existing models and the results are shown in Fig. 5. The results portray that the proposed CSODL-SUAVC model achieved enhanced results with maximum PSNR values for every sample. For instance, in sample 1, the proposed CSODL-SUAVC model demonstrated a maximum PSNR value of 61.229 dB, while AIUAV, CS, and GWO approach produced the least PSNR values such as 60.807, 57.80, and 55.98 dB respectively. Besides, in sample 5, the presented CSODL-SUAVC technique accomplished a maximum PSNR of 57.303 dB, whereas AIUAV, CS, and GWO methodologies produced the minimum PSNR values such as 57.059, 54.99, and 54.10 dB correspondingly.
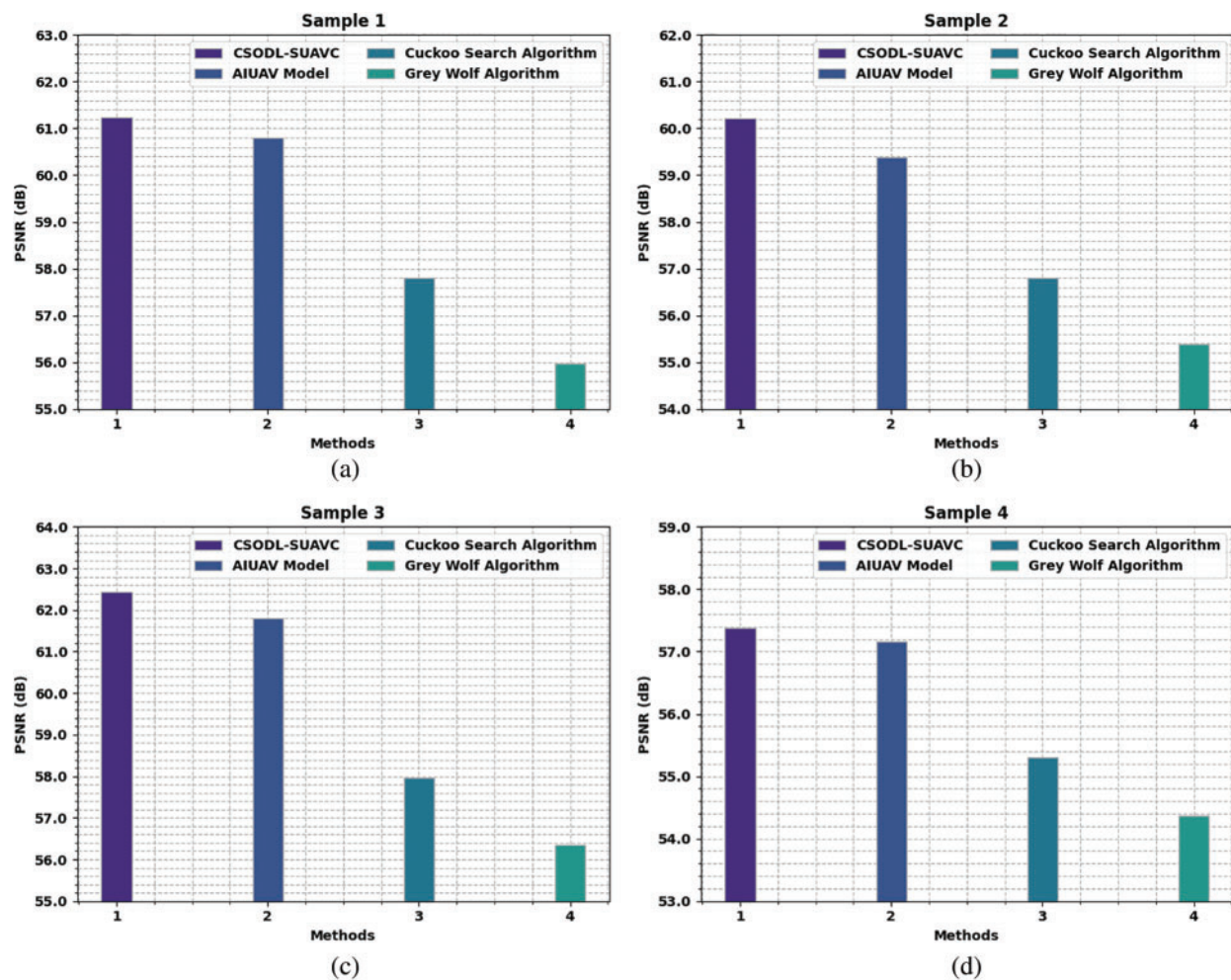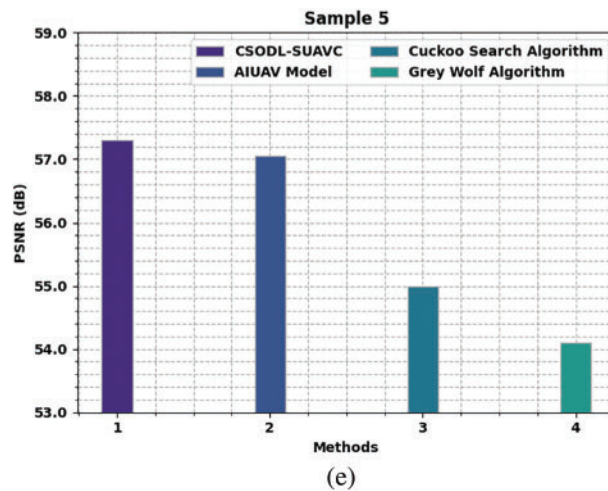

Figure 5: (Continued)

Figure 5: PSNR analysis results of CSODL-SUAVC approach (a) Sampl1, (b) Sample 2, (c) Sample3, (d) Sample4, and (e) Sample5

A comparative CC analysis was conducted between the CSODL-SUAVC approach and other existing methodologies and the results are illustrated in Table 2 and Fig. 6. The outcomes represent that the proposed CSODL-SUAVC approach achieved excellent results with maximal CC values for all the samples. For instance, in sample 1, the proposed CSODL-SUAVC technique demonstrated a maximum CC of 99.95, whereas AIUAV, CS, and GWO algorithms resulted in minimal CC values such as 99.68, 99.46, and 99.29 correspondingly. In addition, in sample 5, the proposed CSODL-SUAVC system exhibited a superior CC of 99.95, whereas AIUAV, CS, and GWO algorithms accomplished less CC values such as 99.79, 99.61, and 99.51 correspondingly.

Table 2: Correlation Coefficient (CC) analysis results of CSODL-SUAVC approach and other existing methodology under distinct test samples

| Test samples	CSODL-SUAVC	AIUAV model	Cuckoo search algorithm	Grey wolf algorithm
Sample 1	99.95	99.68	99.46	99.29
Sample 2	99.93	99.73	99.59	99.45
Sample 3	99.94	99.80	99.58	99.32
Sample 4	99.95	99.72	99.45	99.18
Sample 5	99.95	99.79	99.61	99.51
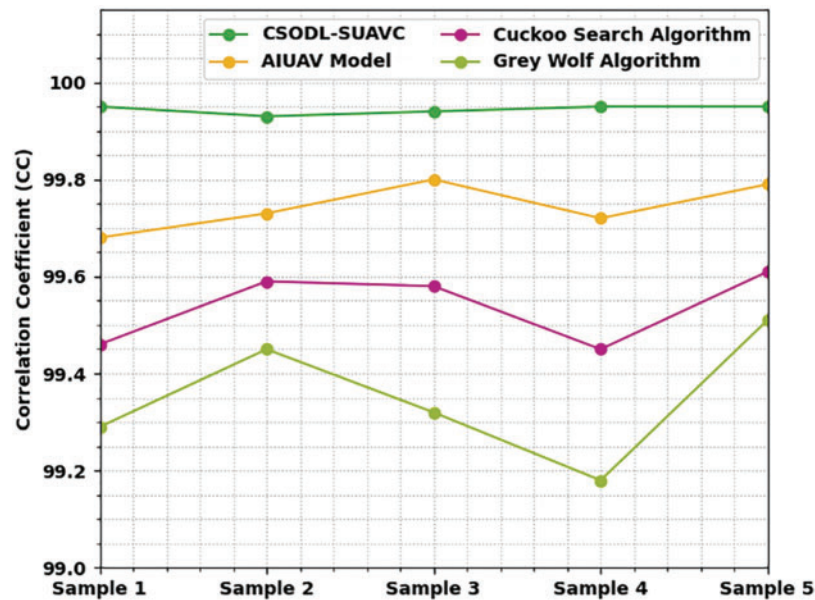
Figure 6: CC analysis results of CSODL-SUAVC approach and other methodologies with distinct test samples

Table 3 and Fig. 7 portray the CT investigation results achieved by the proposed CSODL-SUAVC approach and other recent models under different samples. The figure implies that the proposed CSODL-SUAVC system attained effective outcomes with minimal CT values. For instance, in sample 1, the proposed CSODL-SUAVC algorithm obtained a low CT of 1.115 s, whereas AIUAV, CS, and GWO algorithms achieved high CT values such as 1.735, 2.145, and 2.465 s correspondingly. Eventually, in sample 5, the presented CSODL-SUAVC model offered a low CT of 1.271 s, whereas AIUAV, CS, and GWO algorithms attained maximal CT values such as 1.621, 2.001, and 2.321 s correspondingly.

Table 3: Computational Time (CT) analysis results of CSODL-SUAVC approach and other techniques under distinct test samples

| Test Samples	CSODL-SUAVC	AIUAV Model	Cuckoo Search Algorithm	Grey Wolf Algorithm
Sample 1	1.115	1.735	2.145	2.465
Sample 2	1.231	1.731	2.191	2.581
Sample 3	1.448	1.878	2.178	2.578
Sample 4	1.218	1.798	2.258	2.668
Sample 5	1.271	1.621	2.001	2.321
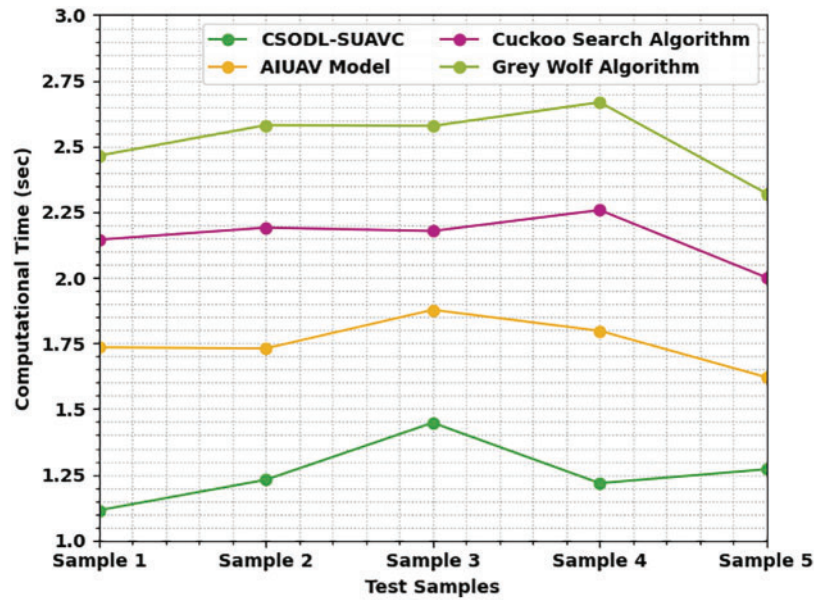
Figure 7: CT analysis results of CSODL-SUAVC approach and other techniques under distinct test samples

Table 4 and Fig. 8 provide an overview of the comparative analysis results accomplished by the proposed CSODL-SUAVC system on the test UCM dataset [28,29]. The results infer that the CSODL-SUAVC model can attain maximum classification results under different measures. For $prec_n$, the proposed CSODL-SUAVC algorithm obtained a high $prec_n$ of 95.66%, whereas BO-SqueezeNet, VGGNet, GoogleNet, ResNetv2, Convolutive Transfer Function based Convolutional Neural Network (CTF-CNN), MobileNetv2, and ResNet models achieved low $prec_n$ values such as 94.59%, 92.73%, 91.58%, 89.69%, 87.77%, 85.88%, and 84.05% respectively.

Table 4: Comparative analysis results of CSODL-SUAVC approach with existing methods under UCM dataset

Methods	Precision	Recall	F1-Score	F2-Score
CSODL-SUAVC	95.66	94.43	95.12	95.68
BO-SqueezzeNet	94.59	93.14	93.43	94.42
VGGNet	92.73	92.73	91.90	92.86
GoogleNet	91.58	91.68	91.09	91.57
ResNetv2	89.69	91.12	89.98	90.67
CTF-CNN	87.77	90.03	88.58	90.16
MobileNetv2	85.88	88.20	86.76	88.69
ResNet	84.05	86.23	85.85	87.79
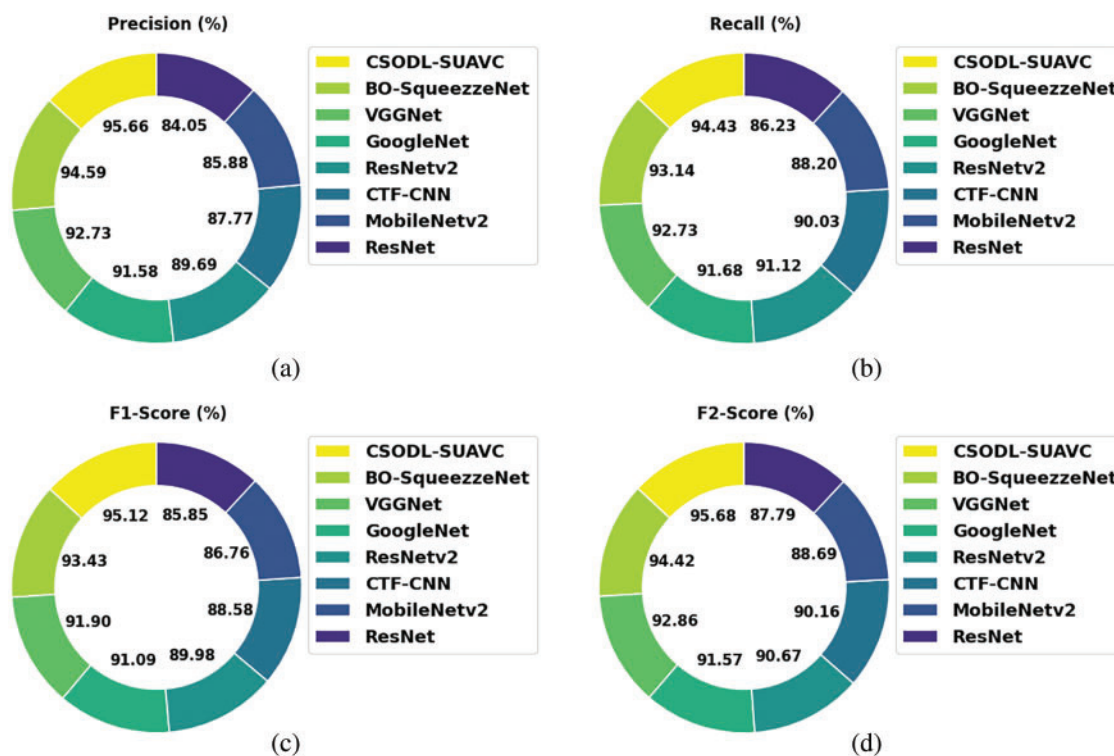
Figure 8: Comparative analysis results of CSODL-SUAVC approach under UCM dataset (a) $Prec_n$, (b) $Reca_l$, (c) $F1_{score}$, and (d) $F2_{score}$

Besides, concerning $F2_{score}$, the proposed CSODL-SUAVC method obtained an improved $F2_{score}$ of 95.68%, whereas BO-SqueezeNet, VGGNet, GoogleNet, ResNetv2, CTF-CNN, MobileNetv2, and ResNet systems achieved low $F2_{score}$ values such as 94.42%, 92.86%, 91.57%, 90.67%, 90.16%, 88.69%, and 87.79% correspondingly.

5 Conclusion

In this study, a new CSODL-SUAVC model has been developed to accomplish secure UAV communication and classification in Industry 4.0 environment. The presented CSODL-SUAVC technique performs image steganography via ML-DWT, CSO-based optimal pixel selection, and signcryption-based encryption technique. At the same time, the image classification module encompasses SRCNN-based feature extraction, Adam optimizer, and softmax classifier. The integration of the CSO-OPS algorithm and Adam optimizer helps in achieving the maximum performance on UAV communication. The proposed CSODL-SUAVC method was experimentally validated using benchmark datasets and the outcomes were measured under distinct aspects. The simulation outcomes infer the better efficiency of the proposed CSODL-SUAVC model over recent approaches. Thus, the presented CSODL-SUAVC model can be applied to enable secure communication and classification in a UAV environment. In the future, hybrid DL methodologies can be applied to improve the classification performance of the proposed CSODL-SUAVC model.

Conflicts of Interest: The authors declare that they have no conflicts of interest to report regarding the present study.

References

[1] D. K. Jain, Y. Li, M. J. Er, Q. Xin, D. Gupta *et al.,* "Enabling unmanned aerial vehicle borne secure communication with classification framework for industry 5. 0," *IEEE Transactions on Industrial Informatics*, vol. 18, no. 8, pp. 5477–5484, 2022.

[2] D. De, A. Karmakar, P. S. Banerjee, S. Bhattacharyya and J. J. Rodrigues, "BCoT: Introduction to blockchain-based internet of things for industry 4.0. in blockchain based internet of things," in: *Blockchain Based Internet of Things, Lecture Notes on Data Engineering and Communications Technologies Book Series*, vol. 112. Singapore: Springer, pp. 1–22, 2022.

[3] K. Dev, K. F. Tsang and J. Corchado, "Guest editorial: The era of industry 5.0—technologies from no recognizable hm interface to hearty touch personal products," *IEEE Transactions on Industrial Informatics*, vol. 18, no. 8, pp. 5432–5434, 2022.

[4] P. F. Lamas, S. I. Lopes and T. M. F. Caramés, "Green IoT and edge AI as key technological enablers for a sustainable digital transition towards a smart circular economy: An industry 5.0 use case," *Sensors*, vol. 21, no. 17, pp. 5745, 2021.

[5] I. Abunadi, M. M. Althobaiti, F. N. Al-Wesabi, A. M. Hilal, M. Medani *et al.,* "Federated learning with blockchain assisted image classification for clustered UAV networks," *Computers, Materials & Continua*, vol. 72, no. 1, pp. 1195–1212, 2022.

[6] B. Chander, S. Pal, D. De and R. Buyya, "Artificial intelligence-based internet of things for industry 4.0," in *Artificial Intelligence-based Internet of Things Systems, Internet of Things*, Cham: Springer, pp. 3–45, 2022.

[7] M. A. Alohali, F. N. Al-Wesabi, A. M. Hilal, S. Goel, D. Gupta *et al.,* "Artificial intelligence enabled intrusion detection systems for cognitive cyber-physical systems in industry 4.0 environment," *Cognitive Neurodynamics*, vol. 16, no. 5, pp. 1045–1057, 2022. https://doi.org/10.1007/s10586-021-03401-5.

[8] D. G. Broo, O. Kaynak and S. M. Sait, "Rethinking engineering education at the age of industry 5. 0," *Journal of Industrial Information Integration*, vol. 25, no. 8, pp. 100311, 2022.

[9] A. M. Hilal, J. S. Alzahrani, I. Abunadi, N. Nemri, F. N. Al-Wesabi *et al.,* "Intelligent deep learning model for privacy preserving IIoT on 6G environment," *Computers, Materials & Continua*, vol. 72, no. 1, pp. 333–348, 2022.

[10] A. V. L. N. Sujith, G. S. Sajja, V. Mahalakshmi, S. Nuhmani and B. Prasanalakshmi, "Systematic review of smart health monitoring using deep learning and artificial intelligence," *Neuroscience Informatics*, vol. 2, no. 3, pp. 100028, 2022.

[11] A. M. Hilal, M. A. Alohali, F. N. Al-Wesabi, N. Nemri, H. J. Alyamani *et al.,* "Enhancing quality of experience in mobile edge computing using deep learning based data offloading and cyberattack detection technique," *Cluster Computing*, vol. 76, no. 4, pp. 2518, 2021. https://doi.org/10.1007/s10586-021-03401-5.

[12] S. A. A. Hakeem, H. H. Hussein and H. Kim, "Security requirements and challenges of 6G technologies and applications," *Sensors*, vol. 22, no. 5, pp. 1969, 2022.

[13] P. Porambage, G. Gur, D. P. M. Osorio, M. Livanage and M. Ylianttila, "6G security challenges and potential solutions," in *2021 Joint European Conf. on Networks and Communications & 6G Summit (EuCNC/6G Summit)*, Porto, Portugal, pp. 622–627, 2021.

[14] S. Wang, M. A. Qureshi, L. M. Pechuaán, T. H. The, T. R. Gadekallu *et al.,* "Explainable AI for B5G/6G: Technical aspects, use cases, and research challenges," arXiv preprint arXiv: 2112. 04698, 2021.

[15] P. K. R. Maddikunta, Q. V. Pham, B. Prabadevi, N. Deepa, K. Dev *et al.,* "Industry 5.0: A survey on enabling technologies and potential applications," *Journal of Industrial Information Integration*, vol. 26, no. 2, pp. 100257, 2022.

[16] R. Sharma and R. Arya, "UAV based long range environment monitoring system with Industry 4.0 perspectives for smart city infrastructure," *Computers & Industrial Engineering*, vol. 168, pp. 10806, 2022.

[17] S. A. Bhat, N. F. Huang, I. B. Sofi and M. Sultan, "Agriculture-food supply chain management based on blockchain and IoT: A narrative on enterprise blockchain interoperability," *Agriculture*, vol. 12, no. 1, pp. 40, 2021.

[18] A. A. Fanid, M. Dabaghchian, N. Wang, P. Wang, L. Zhao *et al.,* "Machine learning-based delay-aware UAV detection over encrypted wi-fi traffic," in *2019 IEEE Conf. on Communications and Network Security (CNS)*, Washington, D.C., USA, pp. 1–7, 2019.

[19] A. Aldaej, T. A. Ahanger, M. Atiquzzaman, I. Ullah and M. Yousufudin, "Smart cybersecurity framework for IoT-empowered drones: Machine learning perspective," *Sensors*, vol. 22, no. 7, pp. 2630, 2022.

[20] Q. A. Al-Haija and A. Al Badawi, "High-performance intrusion detection system for networked UAVs via deep learning," *Neural Computing and Applications*, vol. 34, no. 13, pp. 10885–10900, 2022. https://doi.org/10.1007/s00521-022-07015-9.

[21] R. Kumar, P. Kumar, R. Tripathi, G. P. Gupta, T. R. Gadekallu *et al.,* "SP2F: A secured privacy-preserving framework for smart agricultural unmanned aerial Vehicles," *Computer Networks*, vol. 187, no. 2, pp. 107819, 2021.

[22] K. K. Hasan, U. K. Ngah and M. F. M. Salleh, "Multilevel decomposition discrete wavelet transform for hardware image compression architectures applications," in *2013 IEEE Int. Conf. on Control System, Computing and Engineering*, Penang, Malaysia, pp. 315–320, 2013.

[23] M. H. Qais, H. M. Hasanien, R. A. Turky, S. Alghuwainem, M. T. Véliz *et al.,* "Circle search algorithm: A geometry-based metaheuristic optimization algorithm," *Mathematics*, vol. 10, no. 10, pp. 1626, 2022.

[24] N. Galgali, M. M. Pereira, N. K. Likitha, B. R. Madhushri, E. S. Vani *et al.,* "Real-time image deblurring and super resolution using convolutional neural networks," in *Emerging Research in Computing, Information, Communication and Applications*, Singapore: Springer, pp. 381–394, 2022.

[25] D. Bhowmik, M. Abdullah, R. Bin and M. T. Islam, "A deep face-mask detection model using DenseNet169 and image processing techniques (Doctoral dissertation, Brac University)," 2022.

[26] Y. Yang and S. Newsam, "Bag-of-visual-words and spatial extensions for land-use classification," in *ACM SIGSPATIAL Int. Conf. on Advances in Geographic Information Systems (ACM GIS)*, 2010. [Online]. Available: http://weegee.vision.ucmerced.edu/datasets/landuse.html.

[27] R. L. Ambika, Biradar and V. Burkpalli, "Encryption-based steganography of images by multiobjective whale optimal pixel selection," *International Journal of Computers and Applications*, vol. 46, no. 4, pp. 1–10, 2019.

[28] Y. Li, R. Chen, Y. Zhang, M. Zhang and L. Chen, "Multi-label remote sensing image scene classification by combining a convolutional neural network and a graph neural network," *Remote Sensing*, vol. 12, no. 23, pp. 4003, 2020.

[29] D. Yu, Q. Xu, H. Guo, C. Zhao, Y. Lin *et al.,* "An efficient and lightweight convolutional neural network for remote sensing image scene classification," *Sensors*, vol. 20, no. 7, pp. 1999, 2020.